Journal of Anatomy

J. Anat. (2008) **212**, pp781–794 doi: 10.1111/j.1469-7580.2008.00897.x

The anatomical relationships between the avian eye, orbit and sclerotic ring: implications for inferring activity patterns in extinct birds

Margaret I. Hall

Department of Physiology, Midwestern University, Glendale, Arizona, USA

Abstract

Activity pattern, or the time of day when an animal is awake and active, is highly associated with that animal's ecology. There are two principal activity patterns: diurnal, or awake during the day in a photopic, or high light level, environment; and nocturnal, awake at night in scotopic, or low light level, conditions. Nocturnal and diurnal birds exhibit characteristic eye shapes associated with their activity pattern, with nocturnal bird eyes optimized for visual sensitivity with large corneal diameters relative to their eye axial lengths, and diurnal birds optimized for visual acuity, with larger axial lengths of the eye relative to their corneal diameters. The current study had three aims: (1) to quantify the nature of the relationship between the avian eye and its associated bony anatomy, the orbit and the sclerotic ring; (2) to investigate how activity pattern is reflected in that bony anatomy; and (3) to identify how much bony anatomy is required to interpret activity pattern reliably for a bird that does not have the soft tissue available for study, specifically, for a fossil. Knowledge of extinct avian activity patterns would be useful in making palaeoecological interpretations. Here eye, orbit and sclerotic ring morphologies of 140 nocturnal and diurnal bird species are analysed in a phylogenetic context. Although there is a close relationship between the avian eye and orbit, activity pattern can only be reliably interpreted for bony-only specimens, such as a fossil, that include both measurements of the sclerotic ring and orbit depth. Any missing data render the fossil analysis inaccurate, including fossil specimens that are flat and therefore do not have an orbit depth available. For example, activity pattern cannot be determined with confidence for *Archaeopteryx lithographica*, which has a complete sclerotic ring but no orbit depth measurement. Many of the bird fossils currently available that retain a good sclerotic ring tend to be flat specimens, while three-dimensionally preserved bird fossils tend not to have a well-preserved sclerotic ring or a well-defined optic foramen, necessary for delimiting the orbit depth.

Key words avian; diurnal; eye; fossil; nocturnal; orbit; sclerotic ring; vision.

Introduction

Many aspects of an animal's life history are associated with activity pattern, the time of day when that animal is awake and active. There are two major activity patterns: diurnal, active during the day in a light-rich, or photopic, environment, and nocturnal, active after sunset in a light-limited, or scotopic, environment. 'Scotopic' and 'nocturnal' are interchangeable terms for the purposes of this study, as are 'photopic' and 'diurnal'. Animals may also be crepuscular, active only during dawn and dusk, or cathemeral, equally likely to be active at any time of day. Previous studies on the eye suggest a common organizational principle of how activity pattern is reflected in eye shape: nocturnal birds have a larger corneal diameter relative to the axial length of the eye, probably as an adaptation for increased visual sensitivity to light, while diurnal birds exhibit a larger axial length of the eye relative to the corneal diameter (Hall, 2005; Hall & Ross, 2007; Ross et al. 2007), a shape correlated with increased visual acuity (Martin, 1982, 1990; Ross, 2000; Land & Nilsson, 2002).

Many bony structures are dependent on adjacent soft tissue to achieve their adult shapes, including muscular and other soft tissues. It is reasonable to expect eye size and shape to be correlated with the associated bony anatomy. The sense organs, including the eye, exert a mechanical influence on normal skull morphogenesis (Hanken, 1983; Thorgood, 1988; Hanken & Thorgood, 1993). When eye formation is disrupted in embryonic chicks (Columbre & Crelin, 1957; Tonneyckmuller, 1974; Vanlimborgh & Tonneyckmuller, 1976) and infant humans (Taylor, 1939; Moss & Young, 1960), orbit development is also disrupted. For example, when

Correspondence
Margaret I. Hall, Department of Physiology, Midwestern University, 19555 N 59th Ave, Glendale, AZ 85308, USA. T: +1 623 572 3637; F: +1 623 572 3679; E: margaretihall@yahoo.com

Accepted for publcation *29 February 2008*

microphthalmia (a pathologically small optic globe) occurs naturally or is artificially induced, the orbital structure conforms to the reduced size of the eye, and general facial structure is malformed (Columbre & Crelin, 1957; Tonneyckmuller, 1974; Vanlimborgh & Tonneyckmuller, 1976).

Thus far, primates are the only group for which the relationship between the eye and orbit has been investigated. It has been shown that in small primates the eyeball fills a greater proportion of the orbit than in larger primates (Schultz, 1940). The relationships between activity pattern and bony anatomy have also been investigated in primates, and this information has been utilized for the interpretation of activity pattern for fossil primates. Kay & Cartmill (1977), in the context of an extant comparative base of similarly sized mammals, found that orbital aperture width relative to skull length separates nocturnal and diurnal primates with skull lengths of less than 70 mm. Kay & Kirk (2000) also demonstrated that at small body sizes nocturnal primates exhibit larger orbit diameters than diurnal primates. Heesy & Ross (2001) later showed that, for individuals with skull lengths less than or equal to 65 mm, orbital aperture size can be estimated accurately enough to reconstruct activity pattern in fossil primates from only 10 mm of the orbital rim and an upper molar.

For primates, as mammals, the only bony correlate of eye size and shape is the morphology of the orbit itself. In the absence of the eye, it is only possible to infer the size and shape of that portion of the eye that is directly contained within the orbit, and there is no apparent way to estimate how much of the eyeball protrudes from the bone. Additionally, because with increasing body size primate orbit volumes increase at a greater rate than eye volumes, at larger body sizes dimensions of the orbit do not accurately predict the size or shape of the eye (Schultz, 1940; Kay & Cartmill, 1977; Kay & Kirk, 2000; Heesy & Ross, 2001). Birds, however, like the great majority of diapsids, have an additional bony structure, the sclerotic ring, which houses that portion of the eye that is not contained within the orbit (see Fig. 1; Lemmrich, 1931; Proctor & Lynch, 1993). The sclerotic ring is a series of ossicles in the shape of a ring that is contained within the sclera of the eye, the inner diameter of which surrounds the corneal diameter (see Fig. 1). The exact structure of the sclerotic ring varies across birds in terms of length, degree of curvature, number of ossicles and thickness. It has been hypothesized that information about the soft tissue of the eye can be inferred from the dimensions of the sclerotic ring in ichthyosaurs (Motani et al. 1999; Humphries & Ruxton, 2002; Fernandez et al. 2005), in lizards (Rinehart et al. 2004; Hall, 2005) and in birds (Rowe, 2000; Rinehart et al. 2004). However, to date, the nature of the relationship between hard and soft tissue of the avian eye and orbit has not yet been quantified.

Unlike many mammals, the avian orbit does not contain a fat pad. The only muscles that are present within the orbit proper are the extraocular muscles (Proctor & Lynch, 1993; my personal observation). Although there are several jaw adductor muscles that attach to the ventral-most area of the orbit, these muscles are small and do not protrude significantly into the orbit (Proctor & Lynch, 1993; my personal observation). Therefore, the dimensions of both the orbit and the sclerotic ring may allow for interpretation of the size and shape of the eye when the soft tissue is unavailable for study, as is the case for fossil birds. As the size and shape of the avian eyeball is well correlated with activity pattern (Martin, 1990, 1999; Garamszegi et al. 2002; Hall, 2005; Hall & Ross, 2007; Ross et al. 2007), I hypothesize that the size and shape of the orbit and the sclerotic ring might also be correlated with activity pattern in birds, as has been previously shown to be the case for the eye and orbit in small-bodied primates.

There are three aims to the current study: (1) to quantify the nature of the relationship between the soft-tissue eye and the hard-tissue orbit and sclerotic ring in birds, (2) to investigate how activity pattern is reflected in the bony anatomy associated with the eye, and (3) to identify how much of the bony anatomy is required to interpret activity pattern reliably for a bird that does not have the soft tissue available for study, specifically, for a fossil. For example, *Archaeopteryx lithographica* is an early stem bird species

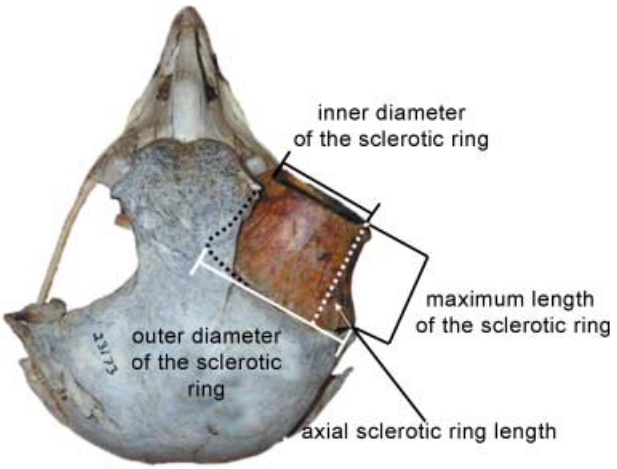

Fig. 1 A superior view of a *Nyctea scandiaca* (snowy owl) skull. On the right the sclerotic ring is present in the orbit; on the left it is absent. The sclerotic ring houses that portion of the eye that protrudes from the orbit. The cornea protrudes laterodistally from the sclerotic ring, and that portion of the sclera that is contained within the orbit proper protrudes proximally. The four measurements taken on the sclerotic ring are here depicted: the inner diameter of the sclerotic ring (the bony correlate of corneal diameter), the maximum length of the sclerotic ring and the axial sclerotic ring length (both bony correlates of that portion of eye that protrudes from the orbit), and the outer diameter of the sclerotic ring. The axial sclerotic ring length was calculated using Pythagoras' theory, with the maximum length of the sclerotic ring as the hypoteneuse of a right-angled triangle and half the inner diameter of the sclerotic ring subtracted from the inner diameter of the sclerotic ring as the base. Solving for the remaining side yields the axial sclerotic ring length.

and as such is of interest to many palaeontologists as part of the investigation into the ecological context of avian evolution. *A. lithographica* is not a crown taxon, and is therefore not suitable for Witmer's 'first-order' fossil interpretation, whereby a fossil structure can be most robustly interpreted when the fossil taxon is 'bracketed' by two extant species that exhibit the same bony structure and that has the same function in both bracketing species (Witmer, 1995). However, the Berlin specimen of *A. lithographica* retains a very well-preserved sclerotic ring, and there has been some discussion about whether palaeoecological and visual information can be interpreted on this basis (e.g. Rinehart et al. 2004). Most fossils, regardless of taxon, and regardless of age, have some missing data; *A. lithographica* exhibits all of the variables required by this study except one, orbit depth, and is here analysed in the context of the extant comparative database, to determine if there is a possibility for an activity pattern interpretation for a fossil with some missing data.

Materials and methods

Study animals

Data were collected on the eyeballs, orbits and sclerotic rings for 75 specimens of 60 non-passerine bird species (see Table 1). These data were supplemented by hard-tissue-only measurements of 131 specimens of 80 non-passerine bird species (see Table 1). Study groups included Strigiformes (barn owls and true owls), Psittaciformes (parrots), Columbiformes (pigeons), Apodiformes (swifts), Falconiformes (falcons), Accipitridrae (hawks), Caprimulgidae (nightjars), Aegothelidae (owlet-nightjars), Nyctibidae (potoos), Podargidae (frogmouths), Charadriiformes [shorebirds (hard tissue measurements only)], and three groups of ratites [ostriches, cassowaries (hard-tissue measurements only) and tinamous (hard-tissue measurements only)]. One fossil bird was included in this study, the Berlin specimen of *A. lithographica,* which has a complete sclerotic ring but no orbit depth. Specimens were obtained from the Departments of Ornithology of the American Museum of Natural History (New York), the Field Museum of Natural History (Chicago) and the British National Museum of Natural History (Tring, UK). *A. lithographica* was measured from a plaster cast at the National Museum of Natural History (Washington, DC). One frozen ostrich specimen was obtained from the Witmer Lab at Ohio University (Athens, OH). All of the other wet specimens were preserved in ethanol, and individuals exhibiting any pathology or unusual preservational deformation were excluded from this study.

Measurements

Soft tissue

Measurements follow Ritland (1982) and Hall & Ross (2007) as follows. For alcohol-preserved specimens, in order to gain access to the eyeball, the eyelid was reflected or removed and the eye was removed from the orbit via blunt dissection using closed, curved scissors and forceps to preserve the eye from accidental puncture. After removal from the orbit, the eyeball was cleaned of all extraocular muscles and remaining fascia, and was inflated using a small amount of preservative injected by a syringe inserted on an angle into the sclera just inferior to the outer edge of the sclerotic ring. Preservative was injected until the eye was fully inflated and would not accept any additional liquid. At that point, maximum corneal diameters and maximum axial lengths of the eye were measured with digital calipers to 0.01 mm. For many of the larger specimens, this required several injections, in which case care was taken to utilize the same puncture hole each time. Any eye that could not be fully inflated was not measured.

Hard tissue

In wet specimens, the orbit was cleaned of fascia and extraocular muscles to allow for clear identification of all bony landmarks. Otherwise, measurements of hard tissue were identical in wet specimens and in dry skulls.

The sclerotic ring cannot be separated from the eye in wet specimens, but in prepared skulls the sclerotic ring is a separate structure from the rest of the skull and is therefore measured independently. All measurements were taken with digital calipers to the nearest 0.01 mm (see Fig. 1). Maximum supero-inferior orbital diameter was measured from the dorsal frontal bone to the quadratojugal. Orbit depth was measured using the depth gauge of the digital calipers from the position of the maximum orbital diameter to the optic foramen (see Fig. 2). If the specimen was too large for the distal end of the calipers to span the orbital diameter, a ruler was placed in the position of the maximum orbital diameter, and the orbit depth was measured from the midpoint of the ruler to the optic foramen. The thickness of the ruler was subtracted from the depth measurement. Head length was measured from the centrepoint of the junction of the beak and skull to inion (posteriormost point on the skull). On the sclerotic ring, maximum inner diameter, maximum outer diameter and maximum length were measured. In most birds the maximum length of the sclerotic ring is obliquely orientated to the visual axis of the eye and therefore may not accurately measure that portion of the axial length of the eye that is housed by the sclerotic ring. Therefore, an additional measurement of sclerotic

Fig. 2 Measurements taken on the orbit. Orbit diameter was measured from (1) that point on the quadratojugal that represents the inferior-most place on the orbital margin to (2) that point on the frontal bone directly opposite point 1. Orbit depth was measured with the caliper depth gauge from the line identified as the orbit diameter to the optic foramen.

Table 1 Species means raw data (all measurements in mm)

Taxon	Activity pattern	*n* wet	*n* dry	Orbit depth	Orbit diameter	Sclerotic ring inner diameter	Sclerotic ring max. length	Axial sclerotic ring length	Corneal diameter	Axial length	Head length
Strigiformes											
*Athene noctua**	photopic	2	1	10.28	18.92	12.46	7.95	7.01	11.52	18.27	52.90
*Athene brama**	photopic	2		7.30	18.90	10.99	7.23	5.71	10.92	17.11	46.75
*Glaucidium brasilianum**	photopic	1	1	8.57	19.73	11.95	8.26	7.54	11.44	18.05	47.73
Glaucidium perlatum	photopic	1		7.89	16.99	10.97	7.63	6.82	10.97	16.80	31.38
Glaucidium jardinii	photopic	1		6.38	14.55	7.91	6.73	5.90	7.91	11.92	27.74
Glaucidium tephronatum	photopic		1	8.69	15.54	8.99	5.24				30.04
Bubo africanus	scotopic	2		15.64	29.28	20.19	14.19	14.11	17.58	23.03	43.86
*Bubo bubo**	scotopic	1		21.86	35.58	23.23	19.14	17.80	20.15	33.95	61.23
*Bubo virginianus**	scotopic		4	18.39	38.61	23.49	18.62	17.93			57.08
Strix aluco	scotopic	2	3	16.17	25.25	17.80	12.94	12.16	15.35	24.96	67.01
*Strix varia**	scotopic		4	13.49	29.40	17.24	11.49	9.90			47.56
Strix occidentalis	scotopic		1	14.28	29.65	18.52	11.58	10.09			48.66
*Nyctea scandiaca**	photopic		1	19.91	32.29	21.33	19.87	18.58			56.02
*Otus scops**	scotopic	2		8.00	16.76	10.94	6.48	5.75	9.86	13.78	41.42
*Otus asio**	scotopic	1	1	9.59	22.75	14.42	10.83	9.85	13.76	20.04	46.01
Otus rutilis	scotopic	1		8.77	19.22	12.72	8.50	7.61	12.72	17.24	32.39
Otus longicornis	scotopic	1		8.00	19.59	11.78	8.33	7.58	11.78	17.89	29.21
*Tyto alba**	scotopic	5	4	10.62	18.67	12.01	7.21	7.13	11.24	17.80	63.90
Asio flammeus	scotopic		3	9.39	19.70	12.41	6.97				60.30
Asio otus	scotopic		3	10.01	19.61	13.18	5.86	5.33			60.42
Ketupa ketupa	scotopic		1	15.59	29.65	16.62	11.48	9.64			47.47
Ketupa zeylonensis	scotopic		1	16.26	32.95	20.07	11.55	9.39			50.19
Scotopelia peli	scotopic		1	21.27	34.41	22.68	12.72	6.76			102.62
*Surnia ulula**	scotopic		1	14.24	21.95	12.13	8.59				40.03
Podargidae											
*Podargus strigoides**	scotopic	1	1	18.43	25.40	15.06	9.73	6.40	14.11	20.23	71.34
Aegothelidae											
*Aegotheles insignis**	scotopic	1		3.37	13.66	8.06	4.93		8.09	9.27	21.87
Nyctibidae											
*Nyctibius griseus**	scotopic	1		11.26	24.21	17.48	5.93	5.28	17.48	19.24	34.35
Caprimulgidae											
*Caprimulgus europaeus**	scotopic	1	1	7.04	13.85	10.71	3.38	2.96	9.77	12.06	38.86
*Caprimulgus macrurus**	scotopic	1	1	5.88	15.50	10.61	2.97	2.20	10.61	12.95	34.06
Caprimulgus madagascariensis	scotopic	1		7.90	14.11	9.02	3.36	2.54	9.02	11.42	23.55
Caprimulgus pectoralis	scotopic		1	6.16	14.36	8.26	2.91	1.60			39.84
Macrodiperyx vexillaria	scotopic		1	8.39	16.25	10.41	2.27	1.81			39.67
Panyptila sanctiheironymi	scotopic		1	5.41	13.05	6.13	2.02	1.45			34.18
Uropsalis segmentata	scotopic	1		4.71	13.96	10.75	3.28	3.05	10.75	11.85	22.16
Eurostopodus macrotis	scotopic	1		11.98	20.42	13.99	5.58	4.42	13.99	18.41	27.71
Hydropsalis climacocerca	scotopic	1		5.72	11.91	7.77	2.97	2.35	7.77	9.58	20.02
*Nyctidromus albicollis**	scotopic	1		5.56	14.96	10.68	3.71	3.14	10.68	12.25	25.86
Scotornis climacurus	scotopic	1		6.45	12.80	.	2.94	0.00		12.36	20.09
*Podager nacunda**	scotopic	1		9.35	18.84	12.20	4.99	3.73	12.20	14.64	27.63
Nyctiphyrnus ocellatus	scotopic	1		6.23	14.80	8.54	3.64	2.93	8.54	10.33	23.17
Falconiformes											
*Falco sparverius**	photopic	1	3	9.11	15.42	8.20	5.18	1.68	8.20	11.98	35.85
Ictina plumbea	photopic	1		13.84	18.87	9.08	6.64	4.79	9.08	16.81	37.14
Polyborus plancus	photopic		3	18.28	26.90	10.00	4.34	1.30			37.14
Falco columbarius	photopic		3	16.62	16.28	9.78	2.46				44.74
Falco mexicanus	photopic		1	21.69	25.20	13.84	5.29	3.54			70.45
Falco ruficolus	photopic		2	22.39	27.01	22.59	6.19				82.31
*Micrastur glivicollis**	photopic		1	18.16	20.12	11.26	4.75	3.26			54.75
Micrastur semitorquatus	photopic		1	22.25	27.66	13.52	5.40	3.18			70.56
*Microheriax caerulescens**	photopic		2	9.34	11.77	5.84	2.14	1.23			29.94
*Sagittarius serpentarius**	photopic		1	27.46	35.52	12.60	5.84				66.36

Table 1 Continued

Taxon	Activity pattern	*n* wet	*n* dry	Orbit depth	Orbit diameter	Sclerotic ring inner diameter	Sclerotic ring max. length	Axial sclerotic ring length	Corneal diameter	Axial length	Head length
Accipidrae											
Accipiter francesi	photopic	1		11.26	17.75	9.76	7.93	6.94	9.76	15.08	32.58
*Buteo buteo**	photopic		2	17.77	23.24	14.71	7.63				50.55
*Buteo jamaicensis**	photopic		2	19.83	29.71	16.11	9.60				55.87
*Aquila chrysaetos**	photopic		1	24.89	38.01	19.77	9.67				68.18
*Accipiter cooperi**	photopic		2	11.76	21.80	10.99	4.73				40.61
Apodiformes											
Collocalia fuciphaga	photopic	2		4.14	10.11	6.05	4.71	4.38	4.69	8.68	24.06
*Collocalia esculenta**	photopic	3		4.09	7.14	4.37	2.73	2.24	3.91	5.92	20.43
Collocalia brevirostris	photopic	1		4.38	9.55	4.55	2.68		4.55	7.17	14.88
*Apus apus**	photopic	2		6.45	11.93	6.54	3.64	2.49	5.05	9.96	30.48
*Apus barbatus**	photopic	1		5.98	11.99	6.40	4.35	3.39	6.40	10.00	21.33
*Cypsiurius parvus**	photopic	3		4.29	9.12	5.25	4.89	2.66	4.64	7.59	21.16
Cypseloides rutilus	photopic	1		5.53	10.84	5.08	3.97	2.95	5.08	8.34	16.15
Cypseloides phelpsi	photopic	1	1	5.84	11.40	5.18	4.48	3.69	5.18	8.26	19.25
Thalurania glaucopis	photopic	1		3.70	5.68	2.65	1.41	0.69	2.65	3.37	11.34
*Chaetura brachyura**	photopic	1		5.62	10.21	4.78	4.29	3.03	4.78	7.02	17.69
Chaetura cinereiventris	photopic		1	2.34	6.19	4.01	1.75	1.50			21.51
Chaetura pelagica	photopic		1	7.01	10.84	4.43	2.25	1.61			26.79
Campylopterus duidae	photopic	1		4.36	6.37	1.92	1.92	1.29	2.82	4.56	13.27
Heledoya branickii	photopic	1		3.07	6.13	3.08	1.12	0.00	3.08	4.45	11.48
Telacanthura ussheri	photopic	1		5.44	10.11	5.79	3.35	2.52	5.79	8.44	20.83
Psittaciformes											
*Pionus menstruus**	photopic	1	1	11.79	15.98	7.57	4.40	1.10	7.52	10.57	46.12
*Deroptyus accipitrinus**	photopic	1		13.84	17.10	7.22	5.15	2.59	7.22	13.34	47.51
*Poicephalus senagalus**	photopic	1		8.85	13.96	6.65	3.91	2.71	6.65	10.90	38.02
Pyrrhyra rhodogaster	photopic	1		7.05	12.09	5.55	2.64	0.60	5.55	7.98	33.84
*Polytelis alexandriae**	photopic	1		7.09	12.64	5.44	3.02	1.41	5.44	7.74	31.78
Rychpsutta pachyryncha	photopic	1		10.50	14.28	7.68	3.72	2.45	7.68	9.57	51.09
Aratinga weddellii	photopic	1		6.74	12.92	6.08	3.54	2.17	6.08	8.59	33.36
Chalcopsitta atra	photopic	1		7.32	13.70	6.23	3.79	2.27	6.23	10.26	41.87
Loriculus galgulus	photopic		1	6.13	9.31	4.40	0.78	0.00			29.49
Psittacus erithacus timni	photopic		1	11.11	16.72	7.88	0.95	0.00			57.94
*Poicephalus senegalus**	photopic		1	9.67	14.47	6.17	1.53	0.00			46.00
Psittacuse erithacus	photopic		1	12.43	18.34	7.48	1.72	0.00			65.66
Poicephalus cryptoxanthus	photopic		1	6.64	14.74	6.19	1.49	0.00			43.57
*Agapornis canus**	photopic		1	4.70	8.31	3.32	0.77	0.00			29.00
Loriculus philippensis	photopic		1	6.11	9.54	4.86	0.58	0.00			32.48
Psittacula alexandri fasciata	photopic		1	9.03	13.13	6.15	1.47	0.00			47.40
Agapornis nigrensis	photopic		1	5.60	8.13	3.64	0.67	0.00			30.98
Agapornis personata	photopic		1	5.12	10.65	4.65	1.06	0.00			33.45
Agapornis roseicollis	photopic		1	5.74	9.94	4.80	0.68	0.00			33.53
*Psittacula krameri**	photopic		1	8.18	13.76	5.95	0.74	0.00			40.84
Psittacula roseata	photopic		1	7.67	9.91	5.26	0.59	0.00			36.12
Agapornis taranta	photopic		1	6.30	10.54	4.27	1.08	0.00			34.74
Anodorynchus glaucus	photopic		1	16.08	23.20	9.17	1.78	0.00			85.56
Graydidascalus brachyurus	photopic		1	11.34	13.34	7.20	1.35	0.00			99.12
Pionus sordidus	photopic		1	12.53	14.89	6.65	1.71	0.00			50.12
Pionites leucogaster	photopic		1	12.38	14.07	7.19	1.72	0.00			50.38
Aratinga erythrogenys	photopic		1	13.05	14.76	7.00	0.88	0.00			48.43
Nondayus nenday	photopic		1	9.16	12.56	6.14	0.96	0.00			46.70
Bolborynchus aurifrons	photopic		1	5.54	8.76	4.32	0.69	0.00			29.79
*Aratinga leucopthalmus**	photopic		1	11.38	14.44	6.45	1.19	0.00			51.39
Myopsitta monachus	photopic		1	7.91	10.96	4.94	1.14	0.00			38.09
*Pezoporus wallicus**	scotopic		1	7.94	13.33	6.85	2.47	2.05			26.89

Table 1 Continued

Taxon	Activity pattern	*n* wet	*n* dry	Orbit depth	Orbit diameter	Sclerotic ring inner diameter	Sclerotic ring max. length	Axial sclerotic ring length	Corneal diameter	Axial length	Head length
Columbiformes											
*Turtur afer**	photopic	1		6.47	12.84	5.01	3.47	2.06	5.01	8.28	23.46
*Gallicolumba luzonica**	photopic	1		7.54	14.32	6.22	3.20	0.00	6.22	7.30	28.75
*Lepitola verreauxi**	photopic	1		9.82	14.62	5.98	4.61	2.92	5.98	9.84	32.01
*Geotrygon montana**	photopic	1		6.41	12.65	5.69	3.25		5.69	8.87	26.01
Treron vernans	photopic	1		8.14	13.73	5.76	3.59	2.43	5.76	8.33	28.98
Chalcops indica	photopic	1	2	7.99	13.53	6.23	3.29	1.18	6.23	8.87	25.66
Streptopelia chinensis	photopic	1		6.77	13.74	5.35	3.65	1.96	5.35	8.83	24.82
Pterocles cornata	photopic	1		6.28	13.85	6.73	4.03	2.67	6.73	10.46	29.61
*Columba plumbea**	photopic	1		7.09	13.44	6.24	3.94	2.28	6.24	9.39	30.72
*Streptopelia vinacea**	photopic		1	6.43	12.84	6.07	2.01	0.92			26.48
Leucosarcia melanoleuca	photopic		1	10.73	16.26	7.95	2.71	1.68			32.04
Zenaiela asiatica	photopic		1	6.79	13.64	6.97	2.39	1.35			29.70
Ptilinopus aurantiif	photopic		1	8.51	13.66	6.90	1.93	0.55			30.24
Zenaida macroura	photopic		1	5.40	13.30	6.55	2.03	1.28			26.91
Petrophassa plumifer	photopic		1	5.92	12.43	5.16	2.12	1.28			23.98
Ocyphaps lophotes	photopic		1	8.11	14.39	6.44	2.08	1.32			28.71
Goura victoria	photopic		1	13.19	23.76	10.68	4.62	3.24			47.55
Struthioniformes											
Struthio camellus	photopic	1	2	39.30	47.19	26.41	8.15	6.17	11.53	38.00	94.40
Casuariiformes											
Casuariius sp.*	photopic		1	31.60		19.61	7.28				120.12
Tinamiformes											
Eudromia elegans	photopic		1	6.24	16.77	8.25	3.75	2.60			33.25
*Nothoprocta ornata**	photopic		1	7.68	14.35	7.25	3.13	1.78			29.93
Crypturellus tataupa	photopic		1	7.10	12.19	5.27	2.59	0.81			24.90
Crypturellus noctivagus	photopic		1	9.94	17.57	9.25	3.89	3.09			34.70
Charadriiformes											
Scolopax minor	photopic		2	7.95	14.20	9.03	2.36	1.41			27.09
Scolopax rusticola	scotopic		2	10.27	16.39	9.80	2.38	1.38			29.43
Gallinago gallinago	scotopic		2	4.89	10.84	5.99	1.52	1.26			22.71
*Vanellus tricolor**	photopic		2	8.75	16.88	7.95	3.22	2.30			29.15
Pluvalis dominica	photopic		3	5.73	16.41	8.49	2.51	2.55			28.07
Numenius phaeopus hudsonicus	photopic		2	6.71	16.79	7.45	3.40	1.95			34.94
Charadrius melodus	photopic		1	5.28	12.30	6.66	2.31	1.84			21.66
*Charadrius vociferus**	photopic		3	6.54	14.36	7.47	2.27	1.80			25.15
Burhinus oedicnemus	scotopic		1	8.91	22.38	12.81	4.96	3.80			38.38
*Burhinus bistratus**	scotopic		1	19.26	27.15	15.95	5.35	4.50			45.94
Burhinus capensis	scotopic		1	16.43	25.67	15.28	4.65	3.67			41.19
Burhinus magnirostris	scotopic		2	17.08	26.46	16.27	4.56	4.88			46.39
*Haematops palliatus**	photopic		1	8.99	19.02	9.81	3.52	3.02			33.55

*Included in the phylogeny for phylogenetic independent contrasts.
Raw data for eye dimensions and related hard-tissue variables. All birds were coded for activity pattern from the literature as follows: (1) König et al. (1999) and del Hoyo et al. (2000); (2) Cleere & Nurney (1998); (3) Ferguson-Lees & Christie (2001); (4) Chantler & Driessens (1995); (5) Juniper & Parr (1998); (6) del Hoyo et al. (1997); (7) del Hoyo et al. (1992); (8) del Hoyo et al. (1996). For axial sclerotic ring length measurements, if the cell is blank, the measurement is not present; if '0' is indicated, the sclerotic ring is flat and therefore no length can be calculated.

ring length that is orientated along the axial length of the eye was calculated by treating the maximum length of the sclerotic ring as the hypoteneuse of a right-angled triangle, and half the difference between the outer and inner diameters of the sclerotic ring as the base of this triange. Pythagoras' theorem was then utilized to solve for the other side of the triangle, and the result was termed the 'axial sclerotic ring length' because it is the measurement of the sclerotic ring length that is along the axial length of the eye (Fig. 1).

The Berlin specimen of *A. lithographica* is contained within a flat slab and is two-dimensional. Therefore, orbit depth was not available, but all other hard-tissue measurements were recorded.

Data analysis

Standard statistical analysis

In order to quantify the relationship between hard and soft tissue in the avian eye and orbit, regressions were calculated to determine the strength of the relationship between the (1) corneal diameter and two bony correlates: (a) the inner diameter of the sclerotic ring and (b) the orbit diameter; and (2) the axial length of the eye with five bony correlates: (a) orbit depth, (b) maximum length of the sclerotic ring, (c) axial sclerotic ring length, (d) the orbit depth added to the maximum length of the sclerotic ring, and (e) the orbit depth added to the axial sclerotic ring length.

In order to quantify the relationship between hard tissue and activity pattern, initially each bird species included in this study was categorized by activity pattern from the literature (del Hoyo et al. 1992, 1996, 1997, 2000; Chantler & Driessens, 1995; Cleere & Nurney, 1998; Juniper & Parr, 1998; König et al. 1999; Ferguson-Lees & Christie, 2001). All animals were classified as either nocturnal or diurnal; there are no cathemeral or crepuscular animals included in this study. The inner diameter of the sclerotic ring, the bony correlate of corneal diameter, was then regressed against each of the five bony correlates for the axial length of the eye (orbit depth, maximum sclerotic ring length, axial sclerotic ring length, the orbit depth added to the maximum length of the sclerotic ring, and the orbit depth added to the axial sclerotic ring length) to investigate the nature of the relationship between the variables. Because the nature of the relationship between orbit diameter and head length has been shown to be useful for interpreting activity pattern in primates (Kay & Cartmill, 1977; Heesy & Ross, 2001), this relationship was also quantified in avians. Inner diameter of the sclerotic ring was then also regressed against head length; for mammals, orbit diameter is the only bony correlate of corneal diameter, but in avians, the inner diameter of the sclerotic ring is a significantly closer bony correlate of corneal diameter, and this measurement may be more useful than orbit diameter in interpreting avian activity pattern.

Because measurement error and natural variation affect both dependent and independent variables, reduced major axis (RMA) was the Model II line-fitting technique utilized in the present study; this method does not assume that variance in either variable is more significant, or that one is influencing the other (Ricker, 1984; Rayner, 1985; Plotnick, 1989; Sokal & Rohlf, 1995). Initially, a single RMA line was calculated for each regression, residuals were calculated from that line for all birds plotted, and a one-way ANOVA was calculated comparing nocturnal and diurnal birds. Then, for each pair of variables, two RMA lines were calculated, one for diurnal birds and one for nocturnal birds. The regression lines were then tested for homogeneity, and then analysis of covariance (ANCOVA) was used to interpret differences in elevation for the activity patterns (Sokal & Rohlf, 1995). The two techniques were utilized for two reasons: first, to confirm the ANCOVA results for differences between groups and, second, to compare differences between nocturnal and diurnal animals in situations where the individual nocturnal and diurnal RMA slopes were not homogeneous and therefore not appropriate for ANCOVA analysis to interpret elevational differences between nocturnal and diurnal birds.

Eight one-way ANOVAs were calculated to determine if there was a significant difference between the activity patterns for the single hard-tissue variables, including (1) $\log_{10}$ inner diameter of the sclerotic ring, (2) $\log_{10}$ sclerotic ring maximum length, (3) $\log_{10}$ axial sclerotic ring length, (4) $\log_{10}$ orbit depth, (5) $\log_{10}$ orbit diameter, (6) $\log_{10}$ (orbit depth + maximum sclerotic ring length), (7) $\log_{10}$ (orbit depth + axial sclerotic ring length), and (8) $\log_{10}$ shape ratio of the inner diameter of the sclerotic ring (the bony correlate of corneal diameter) versus orbit depth + sclerotic ring length (a bony correlate of the axial length of the eye). This ratio allows for an examination of the shape of the orbit and sclerotic ring without the influence of size. In order to ensure that the ratio has no remaining relationship with size, the ratio was regressed against head length, the body size variable that was available for all the animals in this study.

Interquartile boxplots were generated for each variable to display the differences between the means and ranges of each activity pattern. Residuals were calculated in Excel, scatter plots, boxplots and ANOVAs were calculated in SPSS 8.0 (Chicago, IL, USA), and regressions and ANCOVAs were calculated in SMATR (Falster et al. 2003).

After all analyses were completed, the measurement values for *A. lithographica* were plotted on all scatter graphs and boxplots that did not involve orbit depth, the one measurement that was not available for the fossil. This was done to compare the fossil with extant animals of known activity pattern to determine if its activity pattern can be interpreted.

Phylogenetic comparative methods

Standard statistical methods assume independent data observations (Sokal & Rohlf, 1995). However, a common character observed in closely related animals may not be independent. Therefore, in order to take phylogeny into account, this study utilizes independent contrast analysis (Felsenstein, 1985; Harvey & Pagel, 1991), performed in the PDAP module of Mesquite (Maddison & Maddison, 2003; Midford et al. 2005). Currently, avian phylogenetic relationships are highly debated and there is no single commonly accepted phylogeny that includes all the animals in this study. Therefore, individual lower taxonomic-level trees were compiled from individual group phylogenies in Iwaniuk (2003), updated by several more recent lower taxonomic-level molecular phylogenies (Dumbacher et al. 2003; Garcia-Moreno et al. 2003; Paton et al. 2003; Thimassen et al. 2003; Poe & Chubb, 2004; Thomas et al. 2004). Of the 140 species included in the present study, it was possible to find group phylogenies that included 45. Whenever more than one possible cladogram was presented in a systematic analysis, the more resolved tree was always chosen. These individual composite lower-level group phylogenies were then assembled into three different large-scale composite phylogenies using Mesquite (Maddison & Maddison, 2003), including one each that reflects the inter-ordinal relationships from Cracraft et al. (2004), Ericson et al. (2006) and Livezey & Zusi (2007). However, even utilizing the best-resolved trees available, some polytomies in the final trees were unavoidable (see supplementary Fig. S1). There is at present contradictory evidence for branch lengths from the fossil record, molecular clock studies and from biogeography (reviewed in Cracraft, 2000; see also Graur & Martin, 2004). However, branch lengths can affect computations of node values in independent contrast analyses and therefore cannot be ignored. Therefore, in this analysis, branch lengths were both set to 1, and also were recalculated in Mesquite following Grafen (1989) and Pagel (1992), as per Blomberg et al. (2003). Contrasts calculated with these different branch lengths was evaluated for the appropriate fit to the tip data following Díaz-Uriarte & Garland (1998).

Results

The vertebrate eye generally scales with negative allometry to body size (Ritland, 1982; Kiltie, 2000; Hall, 2005, 2008; Ross

Table 2 Results for RMA regression analysis (all variables are $\log_{10}$)

Activity pattern	*Y*-variable	*X*-variable	RMA slope	CI	r^2	Significant ANCOVA?
scotopic	inner diameter sclerotic ring	orbit depth + sclerotic ring length	0.717	0.634–0.811	0.858	yes
photopic	inner diameter sclerotic ring	orbit depth + sclerotic ring length	0.975	0.852–1.114	0.551	yes
scotopic	inner diameter sclerotic ring	orbit depth + axial sclerotic ring length	0.451	0.356–0.571	0.474	slopes not homogeneous
photopic	inner diameter sclerotic ring	orbit depth + axial sclerotic ring length	0.724	0.603–0.87	0.243	slopes not homogeneous
scotopic	inner diameter sclerotic ring	sclerotic ring length	0.548	0.466–0.646	0.75	slopes not homogeneous
photopic	inner diameter sclerotic ring	sclerotic ring length	0.651	0.552–0.766	0.329	slopes not homogeneous
scotopic	inner diameter sclerotic ring	axial sclerotic ring length	0.443	0.371–0.528	0.709	slopes not homogeneous
photopic	inner diameter sclerotic ring	axial sclerotic ring length	0.606	0.794–1.069	0.284	slopes not homogeneous
scotopic	inner diameter sclerotic ring	orbit depth	0.753	0.638–0.890	0.741	slopes not homogeneous
photopic	inner diameter sclerotic ring	orbit depth	0.751	0.794–1.069	0.448	slopes not homogeneous
scotopic	orbit diameter	orbit depth	0.71	0.619–0.815	0.824	yes
photopic	orbit diameter	orbit depth	0.77	0.707–0.844	0.812	yes
scotopic	orbit diameter	head length	0.874	0.784–1.023	0.533	yes
photopic	orbit diameter	head length	0.895	0.7–1.092	0.575	yes
both	orbit diameter	head length	0.793	0.626–0.916	0.704	
scotopic	inner diameter sclerotic ring	head length	0.928	0.737–1.168	0.499	yes
photopic	inner diameter sclerotic ring	head length	1.068	0.911–1.251	0.378	yes
both	inner diameter sclerotic ring	head length	1.24	1.03–1.49	0.524	
both	orbit depth + sclerotic ring length	head length	1.03	0.902–1.18	0.747	
both	orbit depth	head length	1.03	0.902–1.18	0.747	
both	sclerotic ring length	head length	1.24	1.05–1.46	0.623	

et al. 2007; Hall & Ross, 2007). However, in the present study, the bony correlates of axial length of the eye (orbit depth, sclerotic ring length and the two variables summed together) scaled nearly isometrically with head length (see Table 2). Orbit diameter and head length scaled with negative allometry, but the inner diameter of the sclerotic ring and head length scaled with positive allometry (see Table 2).

Comparisons between soft and hard tissue

All relationships between soft-tissue variables and their hard-tissue correlates were highly significant ($P < 0.001$) (see Table 3). The corneal diameter and the inner diameter of the sclerotic ring scaled with slight negative allometry, and the axial length of the eye scaled nearly isometrically with both the orbit depth and the orbit depth summed with the sclerotic ring length (see Table 3). However, the axial length of the eye and the sclerotic ring length considered alone scaled with slight negative allometry (see Table 3).

Activity pattern analysis utilizing hard-tissue-only measurements

One-way ANOVA results for the residuals calculated from a single RMA line calculated for both nocturnal and diurnal birds considered together showed significant differences between nocturnal and diurnal birds for all pairs of hard-tissue variables except for the inner diameter of the sclerotic ring (*y*-variable) and the sclerotic ring maximum length or the axial sclerotic ring length (*x*-variable) (see Table 4).

When RMA lines were calculated individually for each activity pattern for each pair of hard-tissue variables, ANCOVA analyses confirmed ANOVA results. There were significant elevational differences between the regression lines for nocturnal and diurnal birds, for those slopes that passed the tests for homogeneity (see Table 2 and Figs 3 and 4).

All one-way ANOVAs performed on single hard-tissue variables showed significant differences between activity patterns, except for $\log_{10}$ sclerotic ring maximum length and $\log_{10}$ axial sclerotic ring length (see Table 5 and Fig. 5). ANOVAs were calculated in SPSS 8.0 (see Table 5).

There was a non-significant correlation between the shape ratio [inner diameter of sclerotic ring/(orbit depth + sclerotic ring length)] and head length, suggesting that this ratio can be utilized to examine shape differences between the activity patterns with no significant remaining relationship with size ($P = 0.017$, $r^2 = 0.041$).

Phylogenetic correction

Branch length diagnostics generated in PDAP from the all = 1, Grafen (1989) and Pagel (1992) algorithms demonstrated that each of these had the requisite lack of fit between tree topology, branch lengths and tip data (Díaz-Uriarte &

Table 3 Results for comparisons between hard and soft tissue

Soft-tissue variable	Hard-tissue variable	*P*-value	r^2	RMA slope	CI	Phylogenetic independent contrast RMA slope
corneal diameter	inner diameter sclerotic ring	< 0.001	0.936	0.9	0.842–0.963	0.99
corneal diameter	orbit diameter	< 0.001	0.686	1.48	1.28–1.72	
axial length of the eye	orbit depth + sclerotic ring max length	< 0.001	0.836	1.01	0.91–1.13	0.977
axial length of the eye	sclerotic ring max length	< 0.001	0.793	0.889	0.785–0.999	1.008
axial length of the eye	orbit depth + axial sclerotic ring length	< 0.001	0.526	0.633	0.527–0.76	
axial length of the eye	axial sclerotic ring length	< 0.001	0.678	0.609	0.524–0.709	
axial length of the eye	orbit depth	< 0.001	0.694	0.994	0.855–1.156	0.777

Summary results for comparisons between soft-tissue variables and their hard-tissue correlates.

Table 4 Summary results of residual analyses between activity patterns

Y-variable	*X*-variable	RMA Regression Equation	ANOVA *P*-value	ANOVA *F*-value
sclerotic ring inner diameter	orbit depth + sclerotic ring length	$y = (1.2)(x) - 0.49$	< 0.001	11.658
sclerotic ring inner diameter	orbit depth + axial sclerotic ring length	$y = (0.644)(x) + 0.307$	< 0.001	25.571
sclerotic ring inner diameter	sclerotic ring maximum length	$y = (0.997)(x) + 0.231$	0.216	1.546
sclerotic ring inner diameter	axial sclerotic ring length	$y = (0.7)(x) + 0.66$	0.227	1.47
sclerotic ring inner diameter	orbit depth	$y = (1.38)(x) - 0.34$	< 0.001	18.861
sclerotic ring inner diameter	head length	$y = (1.24)(x) - 0.946$	< 0.001	33.168
orbit diameter	orbit depth	$y = (0.888)(x) - 0.946$	< 0.001	13.902
orbit diameter	head length	$y = (0.973)(x) - 0.016$	0.002	9.883

Summary results for the ANOVA analyses of residuals calculated from a single RMA line. A significant ANOVA *P*-value indicates a significant difference between nocturnal and diurnal activity patterns. All variables produced a significant ANOVA except for when measurements of the sclerotic ring are considered alone, indicating that activity pattern can not be interpreted from an isolated sclerotic ring with no other information.

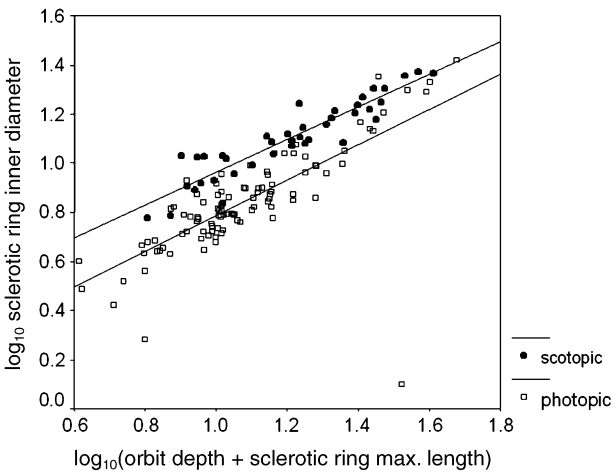

Fig. 3 Scatter plot of $\log_{10}$ inner diameter of the sclerotic ring (bony correlate of corneal diameter) on the *y*-axis and $\log_{10}$(orbit diameter + sclerotic ring max. length) on the *x*-axis (a bony correlate of axial length of the eye). ANCOVA analysis shows significant elevational differences between scotopic and photopic RMA regression lines.

Garland, 1998). Visual examination of the effects of each of these branch length transformations on the contrast data suggested that the Pagel (1992) algorithm best suited the analysis (see Midford et al. 2005). Phylogenetically corrected analyses of the morphological variables described above for the Cracraft et al. (2004) and Livezey & Zusi (2007) phylogenies revealed non-significant differences between the two activity patterns except for the inner diameter of the sclerotic ring (Cracraft et al. 2004: Spearman's rho = 0.598, $P = 0.005$, 20 contrasts reflecting change between activity patterns; Livezey & Zusi, 2007: Spearman's rho = 0.588, $P = 0.02$, 17 contrasts reflecting change between activity patterns). Similar analyses for the Ericson et al. (2006) phylogeny were all non-significant.

Activity pattern interpretation for *A. lithographica*

As seen in Figs 4 and 5, measurements from the Berlin specimen of *A. lithographica* plot within the ranges of both nocturnal and diurnal birds. Therefore, no activity pattern determination can be made based on the available information for *Archaeopteryx*.

Discussion

Comparisons between soft and hard tissue

There is a strong relationship between the avian eye, orbit and sclerotic ring, which underlines the importance of the

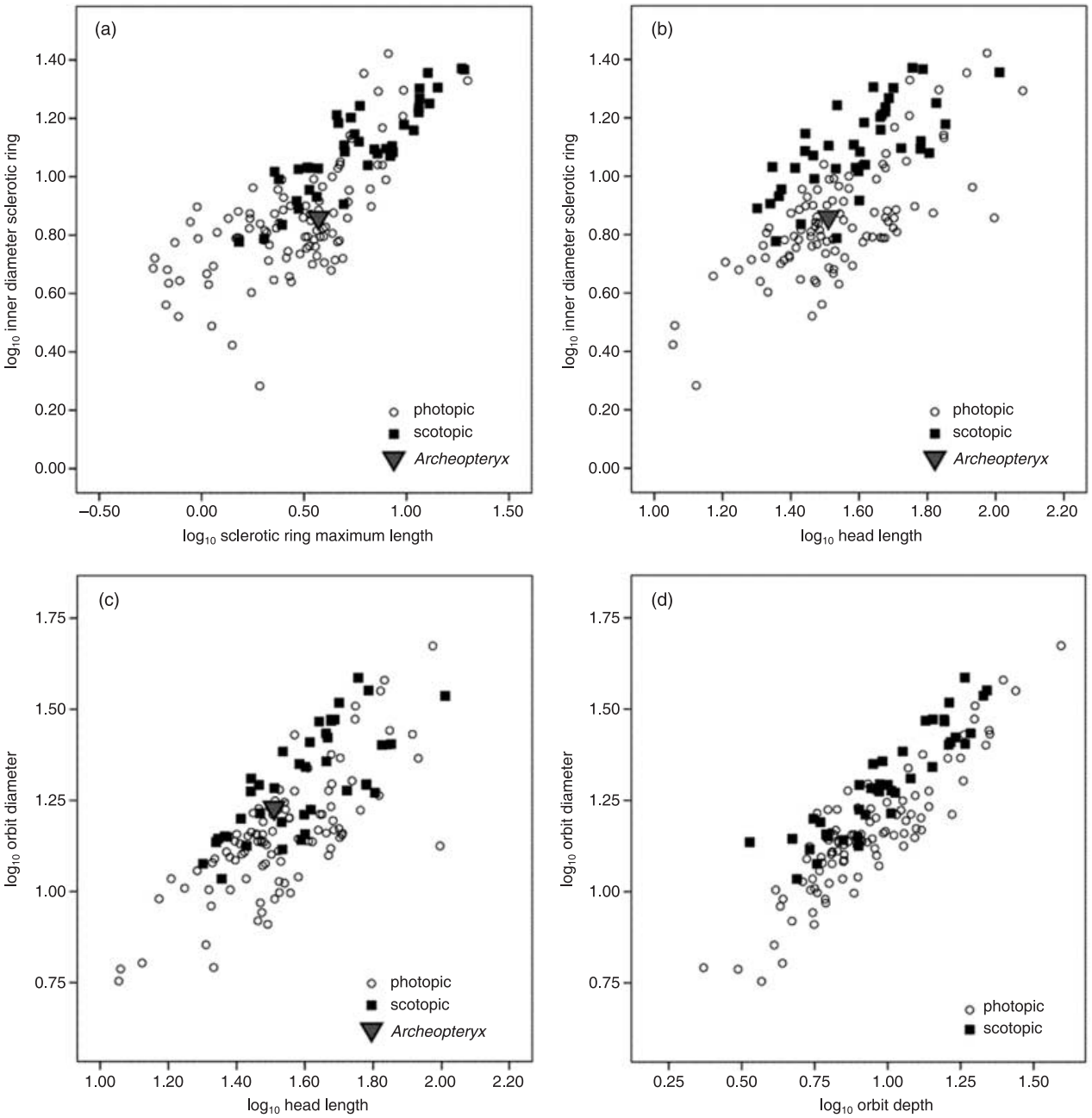

Fig. 4 Three scatter plots, all of which show significant overlap between nocturnal and diurnal birds, with *Archaeopteryx* within the range of both activity patterns: (a) scatter plot of $\log_{10}$ inner diameter of the sclerotic ring (bony correlate of corneal diameter) on the *y*-axis and $\log_{10}$ sclerotic ring maximum length on the *x*-axis (a bony correlate of axial length of the eye); (b) scatter plot of $\log_{10}$ inner diameter of the sclerotic ring (a bony correlate of corneal diameter) on the *y*-axis and $\log_{10}$ head length on the *x*-axis; (c) scatter plot of $\log_{10}$ orbit diameter (a bony correlate of corneal diameter) on the *y*-axis and $\log_{10}$ head length on the *x*-axis; (d) scatter plot of $\log_{10}$ orbit diameter (a bony correlate of corneal diameter) on the *y*-axis and $\log_{10}$ orbit depth on the *x*-axis (a bony correlate of axial length of the eye; note: *Archaeopteryx* is not included in this plot because orbit depth is not available). ANCOVA analyses show significant elevational differences between nocturnal and diurnal RMA regression lines (not depicted); however, there is still sufficient overlap between nocturnal and diurnal activity patterns so as to make fossil interpretation difficult or impossible.

visual system to the evolution of the avian skull. Many of the RMA slopes between a soft-tissue variable and its bony correlate indicate relationships that either include or are near isometry. The corneal diameter is virtually identical to the inner diameter of the sclerotic ring (see Fig. 1); the relationship is highly significant ($P < 0.001$) and nearly all of the variance is explained with an r^2 of 0.936. Therefore, the inner diameter of the sclerotic ring is a useful correlate of the corneal diameter for birds in which the soft tissue is unavailable for study, i.e. specifically for fossil birds.

Table 5 Results for ANOVA analyses (all variables are $\log_{10}$)

Variable	*n*	Mean	SD	df	*F*-variable	*P*-value
inner diameter sclerotic ring*	137	0.9212	0.2163	136	51.738	< 0.001
orbit depth + axial sclerotic ring length	138	1.0529	0.2302	137	11.428	0.001
sclerotic ring max length	138	0.5388	0.3361	137	27.101	< 0.001
axial sclerotic ring length	98	0.4764	0.3308	97	23.362	< 0.001
orbit depth	138	0.9503	0.2185	137	2.382	0.125
orbit diameter	137	1.1972	0.1739	136	22.301	< 0.001
orbit depth + sclerotic ring length	138	1.1108	0.2199	137	10.197	0.002
shape ratio**	137	−0.1908	0.1041	136	47.438	< 0.001

Results for ANOVA analyses. These ANOVAS compare means of nocturnal and diurnal animals to determine if univariate variables can differentiate between the activity patterns.
*This is the only variable with significant results for the phylogenetic independent contrast analysis.
**The shape ratio = $\log_{10}$(inner diameter sclerotic ring – [orbit depth + sclerotic ring length]).

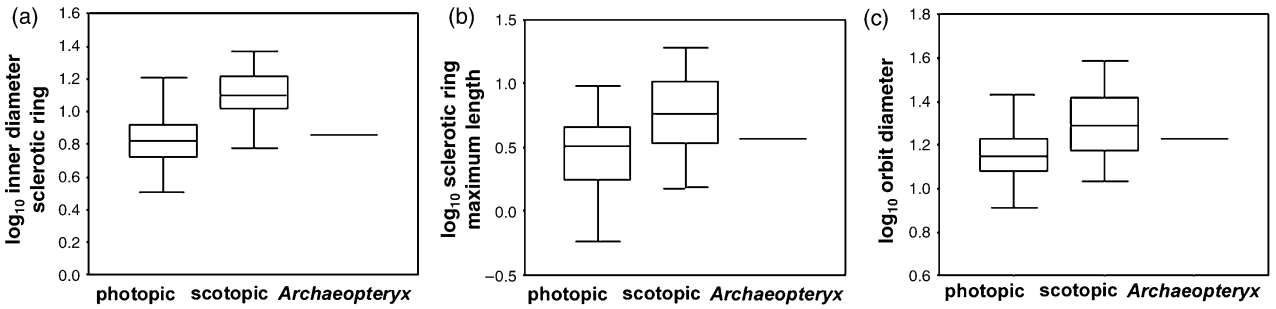

Fig. 5 Quartile boxplot of (a) $\log_{10}$ inner diameter of the sclerotic ring, (b) $\log_{10}$ maximum length of the sclerotic ring and (c) $\log_{10}$ orbit diameter, showing the differences between nocturnal and diurnal activity patterns. For all three plots, the box represents the quartiles, the extensions represent the data range and the solid line represents the mean, and ANOVA analysis found the differences between the means to be statistically significant ($P < 0.001$). *Archaeopteryx* lies within the range of both activity patterns for all three variables.

The axial length of the eye, highly associated with an animal's visual acuity (Hughes, 1977; Land, 1980; Green et al. 1980; Martin, 1982, 1990, 1999), has a significant relationship with both orbit depth ($r^2 = 0.694$), maximum length of the sclerotic ring ($r^2 = 0.793$) and axial sclerotic ring length ($r^2 = 0.547$). However, the relationship between soft and hard tissue is the strongest if the sum of orbit depth and the maximum sclerotic ring length is compared with the axial length of the eye ($r^2 = 0.836$), with an RMA regression slope that indicates isometry. This is logical, as the soft tissue of the eye is only partially housed by either the orbit or the sclerotic ring individually, but when both are considered together, the only portion of the eye without a close bony correlate is that portion of the cornea that protrudes from the inner diameter of the sclerotic ring (see Fig. 1). Interestingly, when the axial sclerotic ring length is considered together with the orbit depth, relatively little of the variance is explained ($r^2 = 0.362$). This may be because as this measurement is calculated from two measurements, both of which have measurement error, rather than collected directly from bony specimens, measurement error is exacerbated. Additionally, as it was not possible to calculate the axial sclerotic ring length for specimens with flat sclerotic rings, the orbit depth alone was used to calculate statistics for many diurnal birds, including most Columbiformes (see Table 1). It may be that there was a reduction in variance explained given that for those animals there was a portion of the axial length of the eye that did not have a bony correlate that was partially compensated for by the use of the maximum sclerotic ring length.

Activity pattern analysis utilizing hard-tissue-only measurements and interpretation of *A. lithographica*

Soft-tissue-only analysis has shown that the size and shape of a bird's eyeball reflect its activity pattern: nocturnal birds have a larger corneal diameter relative to the axial length of the eye, and diurnal birds have a larger axial length of the eye relative to the corneal diameter (Ritland, 1982; Martin, 1999; Hall, 2005; Hall & Ross, 2007; Ross et al. 2007). This study shows that when all the hard-tissue variables are available for analysis, it is possible to infer the size and shape of the eyeball, and that these hard-tissue variables are well associated with the bird's activity pattern.

Analysis of phylogenetically independent contrasts did not show significant differences between nocturnal and diurnal birds for any of the variables except the inner diameter of the sclerotic ring. PIC analysis of the relevant

soft-tissue variables, i.e. corneal diameter and axial length of the eye, also did not find these size variables to be statisistically different between activity patterns (Hall, 2005; Hall & Ross, 2007). However, the $\log_{10}$ shape ratio of corneal diameter versus axial length of the eye was found previously to be highly significantly different for birds with different activity patterns (Hall, 2005; Hall & Ross, 2007). Here the equivalent bony shape ratio, the $\log_{10}$ ratio of the inner diameter of the sclerotic ring/(sclerotic ring length + orbit depth), was not found to be significant in a phylogenetic context. However, this may be because the hard-tissue sample size in the present study (45 species) is significantly smaller than the soft-tissue sample size (202 species: Hall, 2005; Hall & Ross, 2007). Therefore, a PIC analysis of the shape ratio may be significant for an increased hard-tissue sample size.

In standard statistical analysis, ANOVA analyses of residuals show a significant difference between the means of nocturnal and diurnal birds, indicating that all hard-tissue variables are statistically capable of differentiating between the activity patterns except measurements of the sclerotic ring alone. These results are confirmed by the ANCOVA analyses of elevational differences between RMA regression lines for nocturnal and diurnal birds. Also, all ANOVA analyses of these individual hard-tissue variables show statistically significant differences between the means of nocturnal and diurnal animals. However, not all the hard-tissue variables are equally capable of separating nocturnal and diurnal birds. One aim of the present study was to see how much bony anatomy is required to interpret activity pattern reasonably, especially to do so for fossils that are usually incomplete specimens. Just dimensions of the sclerotic ring alone do not separate nocturnal and diurnal birds well (Fig. 4). Also, a scatter plot of just orbital dimensions, orbit diameter on the *y*- and orbit depth on the *x*-axis, reveals considerable overlap between nocturnal and diurnal birds (Fig. 4). The best separation between nocturnal and diurnal birds in scatter plots is when dimensions of both orbit depth and sclerotic ring are available (Fig. 3). Therefore, although the Berlin specimen of *A. lithographica* preserves many of the variables included here, including the inner diameter of the sclerotic ring, maximum sclerotic ring length, orbit diameter and head length, orbit depth and axial sclerotic ring length are unavailable. Inner diameter of the sclerotic ring and the maximum length of the sclerotic ring are insufficient to interpret activity pattern: the fossil plotted within the ranges of both nocturnal and diurnal birds for all available variables, and thus activity pattern cannot be reliably interpreted (Figs 4 and 5).

The measurements that have been useful for primate activity pattern studies, orbit diameter and skull length (Kay & Cartmill, 1977; Heesy & Ross, 2001), are not useful for birds. Although there is a significant ANCOVA between nocturnal and diurnal birds, the scatter plot shows extensive overlap between the two activity patterns (see Fig. 4c). The inner diameter of the sclerotic ring on the *y*-axis and head length on the *x*-axis shows better separation between nocturnal and diurnal birds (see Fig. 4b). This is logical because there is a much closer relationship between corneal diameter and inner diameter of the sclerotic ring than there is with orbit diameter. However, there is still significant overlap between nocturnal and diurnal birds, and head length is not as useful as direct measurements of orbit depth and sclerotic ring for interpreting activity pattern in birds.

Although all ANOVA analyses of these hard-tissue variables show statistically significant differences between the means of nocturnal and diurnal animals, the boxplots in Fig. 5 all show single variables with considerable overlap in range between the activity patterns, and fossil interpretation would only be possible for a bird that plotted in the extremes. The single variable with the best separation between nocturnal and diurnal animals is the inner diameter of the sclerotic ring, the bony correlate of the corneal diameter, which in turn is highly associated with visual sensitivity (Fig. 5). This is also the only hard-tissue variable that phylogenetically independent contrast analysis found to be significantly different between nocturnal and diurnal birds in two of the three tree topologies analysed. However, the inner diameter of the sclerotic ring still shows considerable overlap between the activity patterns, and, as discussed above, *Archaeopteryx* plots within the ranges of both activity patterns. For the great majority of the birds in this sample, an isolated sclerotic ring is not sufficient to interpret activity pattern reliably, nor are dimensions of just the sclerotic ring and the orbit diameter, and studies that attempt to do so (e.g. Rinehart et al. 2004) are not robust. Except for those birds that plot in the extremes of the nocturnal and diurnal ranges, dimensions of both the sclerotic ring and orbit depth are necessary to make a reliable activity pattern interpretation.

It would be a great advance in understanding the evolution and palaeoecologies of birds if activity pattern could be interpreted from bony variables alone. However, most bird fossils found thus far are incomplete in some way, due at least in part to the fragile nature of bird osteology. Therefore, this important limitation must be considered by bird and non-avian dinosaur palaeontologists because, for the majority of bird fossils currently available, it is not possible to interpret avian palaeo-activity patterns directly from a fossil. However, the present study quantifies scaling relationships between the avian eye, orbit and sclerotic ring, and underlines the importance of the visual system in influencing the evolution of avian skull morphology.

Concluding remarks

This study quantifies the scaling relationships between the hard and soft tissue of the avian eye and orbit, showing that there is a close relationship between the soft tissue

(corneal diameter and axial length of the eye) and hard tissue (the orbit and sclerotic ring). Activity pattern significantly influences the morphology of the orbit and sclerotic ring, just as it influences the soft tissue of the avian eye. Although it is theoretically possible to interpret activity pattern from hard-tissue characteristics alone, not all hard-tissue variables are equally capable of differentiating between nocturnal and diurnal birds. The clearest separation between activity patterns is possible when dimensions of both the sclerotic ring and the orbit depth are considered together. It is not currently possible to interpret the activity pattern of *A. lithographica* reliably, for which orbit depth is not available.

Acknowledgments

For access to specimens, I thank the American Museum of Natural History (New York), the Field Museum of Natural History (Chicago), the National Museum of Natural History, Smithsonian Institution (Washington, DC), the British National Museum of Natural History (Tring, UK), and the Witmer Lab (Athens, OH). I thank my funding sources, including the Society of Integrative and Comparative Biology Grant-in-Aid-of-Research, the Frank M. Chapman Memorial Fund, the Field Museum of Natural History Visiting Scholarship, and the Jurassic Foundation. This work was part of a PhD thesis, and here I thank my advisory committee, including Drs Callum Ross, Matthew Carrano, Susan Evans, Catherine Forster, William Jungers and Nathan Kley. In addition, for helpful comments I thank Drs Joel Cracraft, Andrzej Elzanowski, Christopher Heesy, Keith Metzger, Patrick O'Connor, Maureen O'Leary, F. James Rohlf, Karen Samonds and Lawrence Witmer. For great assistance in figure composition, I thank Dr Beth Townsend. For invaluable assistance in the phylogenetic analysis, I thank Drs Christopher Heesy, Andrew Iwaniuk and Jason Kamilar. Lastly, I thank Dr Julia Clarke and two anonymous reviewers for helpful comments on submitted drafts of the manuscript.

References

Blomberg SP, Garland T Jr, Ives AR (2003) Testing for phylogenetic signal in comparative data: behavioral traits are more labile. *Evolution* **57**, 717–745.

Chantler P, Driessens G (1995) *Swifts: A Guide to the Swifts and Treeswifts of the World*. East Sussex, South Africa: Russel Friedman Books CC.

Cleere N, Nurney D (1998) *A Guide to Nightjars and Related Nightbirds*. New Haven, CT: Yale University Press.

Columbre AJ, Crelin ES (1957) The role of the developing eye in the morphogenesis of the avian skull. *Am J Phys Anthropol* **16**, 25–37.

Cracraft J (2000) Avian evolution, Gondwana biogeography and the Cretaceous-Tertiary mass extinction event. *Proc R Soc Lond B* **268**, 459–469.

Cracraft J, Barker FK, Braun M, et al. (2004) Phylogenetic relationships among modern birds (Neornithes). In *Assembling the Tree of Life* (eds Cracraft J, Donoghue MJ), pp. 468–489. Oxford: Oxford University Press.

Díaz-Uriarte R, Garland T Jr (1998) Effects of branch length errors on the performance of phylogenetically independent contrasts. *Syst Biol* **47**, 654–672.

Dumbacher JP, Pratt TK, Fleischer RC (2003) Phylogeny of the owlet-nightjars (Aves: Aeothelidae) based on mitochondrial DNA sequence. *Mol Phylogen Evol* **29**, 540–549.

Ericson PGP, Anderson CL, Britton T, et al. (2006) Diversification of Neoaves: integration of molecular sequence data and fossils. *Biol Lett* **2**: 543–547.

Falster D, Warton D, Wright I (2003) (S)Matr: Standardized major axis tests and routines. Version 1.0. http://www.bio.mq.edu.au/ecology/SMATR.

Felsenstein J (1985) Phylogenies and the comparative method. *Am Nat* **125**, 1–15.

Ferguson-Lees J, Christie DA (2001) *Raptors of the World*. Boston: Houghton Mifflin.

Fernandez MS, Archuby F, Talevi M, Ebner R (2005) Ichthyosaurian eyes: paleobiological information content in the sclerotic ring of *Caypullisaurus* (Ichthyosauria, Ophthalmosauria). *J Vert Paleontol* **25**, 330–337.

Garamszegi LZ, Moller AP, Erritzoe J (2002) Coevolving avian eye size and brain size in relation to prey capture and nocturnality. *Proc R Soc Lond B* **269**, 961–967.

Garcia-Moreno J, Sorenson MD, Mindell DP (2003) Congruent avian phylogenies inferred from mitochondrial and nuclear DNA sequences. *J Mol Evol* **57**, 27–37.

Grafen A (1989) The phylogenetic regression. *Phil Trans Roy Soc Lond B* **326**, 119–157.

Graur D, Martin W (2004) Reading the entrails of chickens: molecular timescales of evolution and the illusion of precision. *Trends Genet* **20**, 80–86.

Green DG, Powers MK, Banks MS (1980) Depth of focus, eye size and visual acuity. *Vis Res* **20**, 827–835.

Hall MI (2005) *The roles of function and phylogeny in the morphology of the diapsid visual system*. PhD dissertation. Stony Brook, NY: Stony Brook University.

Hall MI, Ross CF (2007) Eye shape and activity pattern in birds. *J Zool* **271**, 437–444.

Hall, MI (2008) Comparative analysis of the size and shape of the lizard eye. *Zoology* **111**, 62–75.

Hanken J (1983) Miniaturization and its effects on cranial morphology in plethodontid salamanders, genus *Thorius* (Amphibia, Plethodontidae): II. The fate of the brain and sense organs and their role in skull morphogenesis and evolution. *J Morph* **177**, 255–268.

Hanken J, Thorgood P (1993) Evolution and development of the vertebrate skull: the role of pattern formation. *TREE* **8**, 9–15.

Harvey PH, Pagel MD (1991) *The Comparative Method in Evolutionary Biology*. Oxford: Oxford University Press.

Heesy CP, Ross CF (2001) Evolution of activity patterns and chromatic vision in primates: morphometrics, genetics and cladistics. *J Hum Evol* **40**, 111–149.

del Hoyo J, Elliott A, Sargatal J (eds) (1992) *Handbook of the Birds of the World. Volume 1, Ostrich to Ducks*. Barcelona: Lynx Ediciones.

del Hoyo J, Elliott A, Sargatal J (eds) (1996) *Handbook of the Birds of the World. Volume 3, Hoatzin to Auks*. Barcelona: Lynx Ediciones.

del Hoyo J, Elliott A, Sargatal J (eds) (1997) *Handbook of the Birds of the World. Volume 4, Sandgrouse to Cuckoos*. Barcelona: Lynx Ediciones.

del Hoyo J, Elliott A, Sargatal J (eds) (2000) *Handbook of the Birds of the World. Volume 5, Barn-Owls to Hummingbirds*. Barcelona: Lynx Ediciones.

Hughes A (1977) The topography of vision in mammals of contrasting life style: comparative optics and retinal organisation. In *The Visual System in Vertebrates* (ed. Crescitelli F), pp. 613–756. Berlin: Springer-Verlag.

Humphries S, Ruxton GD (2002) Why did some icthyosaurs have such large eyes? *J Exp Biol* **205**, 439–441.
Iwaniuk AN (2003) *The evolution of brain size and structure in birds*. PhD Thesis. Clayton, Victoria, Australia: Monash University.
Juniper T, Parr M (1998) *Parrots: A Guide to Parrots of the World*. New Haven, CT: Yale University Press.
Kay RF, Cartmill M (1977) Cranial morphology and adaptations of *Palaechthon nacimienti* and other paromomyidae (plesiadapoidea, ? Primates), with a description of a new genus and species. *J Hum Evol* **6**, 19–35.
Kay RF, Kirk EC (2000) Osteological evidence for the evolution of activity pattern and visual acuity in primates. *Am J Phys Anthropol* **113**, 235–262.
Kiltie RA (2000) Scaling of visual acuity with body size in mammals and birds. *Funct Ecol* **14**, 226–234.
König CC, Weick F, Becking JH (1999) *A Guide to Owls of the World*. New Haven, CT: Yale University Press.
Land MF (1980) Optics and vision in invertebrates. In *Handbook of Sensory Physiology VII/6B* (ed. Antrum H), pp. 471–592. Berlin: Springer-Verlag.
Land MF, Nilsson D-E (2002) *Animal Eyes*. New York: Oxford University Press.
Lemmrich W (1931) Der skleralring der vögel. *Jena Z Naturwiss* **65**, 513–586.
Livezey BC, Zusi RL (2007) Higher-order phylogeny of modern birds (Theropoda, Aves: Neornithes) based on comparative anatomy, II. Analysis and discussion. *Zool J Linn Soc* **149**, 1–95.
Maddison WP, Maddison DR (2003) Mesquite: a modular system for evolutionary analysis. Version 1.05. http://mesquiteproject.org.
Martin G (1999) Optical structure and visual fields in birds: their relationship with foraging behaviour and ecology. In: *Adaptive Mechanisms in the Ecology of Vision* (eds Archer SN, Djamgoz MBA, Loew ER, Partridge JC, Vallerga S), pp. 485–508. London: Kluwer Academic.
Martin GR (1982) An owl's eye: schematic optics and visual performance in *Strix aluco*. *J Comp Physiol* **145**, 341–349.
Martin GR (1990) *Birds by Night*. San Diego: Academic Press.
Midford PE, Garland T Jr, Maddison WP (2005) PDAP package of Mesquite. Version 1.07. http://mesquiteproject.org/pdap_mesquite/.
Moss ML, Young RW (1960) A functional approach to craniology. *Am J Phys Anthropol* **18**, 281–292.
Motani R, Rothschild BM, Wahl W Jr (1999) Large eyeballs in diving ichthyosaurs. *Nature* **402**, 747.
Pagel, MD (1992) A method for the analysis of comparative data. *J Theor Biol* **156**, 431–442.
Paton TA, Baker AJ, Groth JG, Barrowclough GF (2003) RAG-1 sequences resolve phylogenetic relationships within Charadriiform birds. *Mol Phylogenet Evol* **29**, 268–278.
Plotnick RE (1989) Application of bootstrap methods to reduced major axis line fitting. *Syst Zool* **38**, 144–153.
Poe S, Chubb AL (2004) Birds in a bush: five genes indicate explosive evolution of avian orders. *Evolution* **58**, 404–415.
Proctor NS, Lynch PJ (1993) *Manual of Ornithology: Avian Structure and Function*. New Haven, CT: Yale University Press.
Rayner JMV (1985) Linear relations in biomechanics: the statistics of scaling functions. *J Zool Lond* **206**, 415–439.
Ricker WE (1984) Computation and uses of central trend lines. *Can J Zool* **62**, 1897–1905.
Rinehart L, Lucas S, Heckert A, Hunt A (2004) Vision characteristics of *Coelophysis bauri* based on sclerotic ring, orbit, and skull morphology. *J Vert Paleontol* **24** (Suppl. 3): 104A.
Ritland S (1982) *The allometry of the vertebrate eye*. PhD thesis, Chicago: University of Chicago.
Ross CF (2000) Into the light: The origin of Anthropoidea. *Annual Reviews of Anthropology* **29**:147–194.
Ross CF, Hall MI, Heesy CP (2007) Were basal primates nocturnal? Evidence from eye size and shape. In *Primate Origins and Adaptations* (eds Ravosa M, Dagosto M), pp. 233–256. New York: Kluwer Academic/Plenum Publishers.
Rowe MP (2000) Inferring the retinal anatomy and visual capacities of extinct vertebrates. *Palaeontologia Electronica* **3**, 43.
Schultz AH (1940) The size of the orbit and of the eye in primates. *Am J Phys Anthropol* **26**, 389–408.
Sokal RR, Rohlf FJ (1995) *Biometry*, 3rd edn. New York: W. H. Freeman and Co.
Taylor WOG (1939) Effect of enucleation of one eye in childhood on the subsequent development of the face. *Trans Ophthal Soc UK* **59**, 361–371.
Thimassen HA, Wiersema AT, Bakker MAGD, Knijff PD, Hetebrij E, Povel GDE (2003) A new phylogeny of swiftlets (Aves: Apodidae) based on cytochrome-b DNA. *Mol Phylogenet Evol* **29**, 86–93.
Thomas GH, Willis MA, Szekely T (2004) A supertree approach to shorebird phylogeny. *BMC Evol Biol* **4** doi: 10.1186/1471-2148-4-28.
Thorgood P (1988) The developmental specification of the vertebrate skull. *Development* **103** (Suppl.), 141–153.
Tonneyckmuller I (1974) Growth of eyes and orbits in chicken embryo. 8. Development of skull in embryos of 12–17 days with artificially induced bilatera micropthalmia. *Acta Morphol. Neerlando-Scandinavica* **12**, 145–158.
Vanlimborgh J, Tonneyckmuller I (1976) Experimental studies on relationships between eye growth and skull growth. *Ophthalmologica* **173**, 317–325.
Witmer LM (1995) The extant phylogenetic bracket and the importance of reconstructing soft tissues in fossils. In *Functional Morphology in Vertebrate Paleontology* (ed. Thomason JJ), pp. 19–33. New York: Cambridge University Press.

Supplementary material

The following supplementary material is available for this article:

Fig. S1 The three composite phylogenies of birds used to calculate phylogenetically independent contrasts. All three trees contain the same lower taxonomic-level relationships, and differ in their interordinal relationships; (a) reflects interordinal relationships supported by Cracraft et al. (2004), (b) reflects those from Ericson et al. (2006) and (c) reflects those from Livezey & Zusi (2007).

This material is available as part of the online article from: http://www.blackwell-synergy.com/doi/abs/10.1111/j.1469-7580.2008.00897.*x*
(This link will take you to the article abstract).

Please note: Blackwell Publishing are not responsible for the content or functionality of any supplementary materials supplied by the authors. Any queries (other than missing material) should be directed to the corresponding author for the article.